

The Energy Gap Law for Triplet States in Pt-Containing Conjugated Polymers and Monomers

Joanne S. Wilson,[†] Nazia Chawdhury,[†] Muna R. A. Al-Mandhary,[‡] M. Younus,[§] Muhammad S. Khan,[‡] Paul R. Raithby,[§] Anna Köhler,^{*,†} and Richard H. Friend[†]

Contribution from Cavendish Laboratory, University of Cambridge, Madingley Road, Cambridge CB3 0HE, United Kingdom, Department of Chemistry, College of Science, Sultan Qaboos University, Al-Khod 123, Sultanate of Oman, and Department of Chemistry, University of Cambridge, Lensfield Road, Cambridge CB2 1EW, United Kingdom

Received April 17, 2001

Abstract: The energy gap law established for aromatic hydrocarbons and rare earth ions relates the nonradiative decay rate to the energy gap of a transition through a multiphonon emission process. We show that this energy gap law can be applied to the phosphorescence of a series of conjugated polymers and monomers for which the radiative decay rate has been enhanced through incorporation of a heavy metal. We find that the nonradiative decay rate from the triplet state T_1 increases exponentially with decreasing T_1-S_0 gap for the polymers and monomers at 300 and 20 K. Comparison of the nonradiative decay of polymers with that of their corresponding monomers highlights the role of electron–lattice coupling.

I. Introduction

The nonradiative decay of triplet states in aromatic hydrocarbon molecules has been explained both theoretically and experimentally in terms of the well-established energy gap law for unimolecular decay.^{1,2} The mechanism for these nonradiative transitions is controlled by Franck–Condon overlap of wave functions.³ For a series of materials which have similar ground and excited states but with varying triplet energy, an exponential relationship is seen between the rate constant and the energy gap of the transition. This was first suggested as an empirical relationship by Robinson and Frosch⁴ in 1963 and then a more quantitative theory for nonradiative decay in aromatic hydrocarbons was established by Siebrand² in 1967 showing a linear relationship between the log of the Franck–Condon factor and the energy gap of a transition. This work was later extended by other authors who concentrated on the modes by which the nonradiative decay occurs.^{5,6} The energy gap law has also been applied to rare earth ions⁷ and to Pt, Os, and Ru complexes.⁸

However, to our knowledge, the nonradiative decay of triplet states in conjugated polymers has not yet been considered in this context. Yet radiationless transitions are more common than radiative transitions,⁹ so that a knowledge of triplet state decay mechanisms is vital for a full understanding of the photochem-

istry of conjugated polymers. Furthermore, triplet states play an important role in optical and electrical processes within conjugated polymers with direct implications for their technological exploitation. For example, photoluminescence is affected by the relative energies of the singlet and triplet states^{10–12} and the ultimate efficiency of light emitting diodes (LEDs) is controlled by the fraction of triplet states generated^{13–16} or harvested.^{17–19}

Emission from a triplet excited state to a singlet ground state (phosphorescence) is forbidden by spin selection rules, but it can be rendered partially allowed by spin–orbit coupling induced by heavy atoms or vibrational coupling.^{3,20} However, most organic conjugated materials do not contain heavy atoms to contribute to spin–orbit coupling. Vibrational coupling is required for $\pi-\pi^*$ transitions to mix π with σ states to produce a change in orbital angular momentum. This is necessary to compensate the spin flip when crossing from the triplet to the singlet manifold. Suitable modes usually involve an out-of-plane (often C–H) bending or a ring twist.²⁰ For small conjugated molecules such as benzene and naphthalene, the out-of-plane bending modes provide the route by which phosphorescence

* Corresponding author. E-mail: ak10007.cam.ac.uk.

[†] Cavendish Laboratory, University of Cambridge.

[‡] Sultan Qaboos University.

[§] Department of Chemistry, University of Cambridge.

(1) Englman, R.; Jortner, J. *Mol. Phys.* **1970**, *18*, 145.

(2) Siebrand, W. *J. Chem. Phys.* **1967**, *47*, 2411.

(3) Turro, N. J. *Modern Molecular Photochemistry*; University Science Books: Mill Valley, CA, 1991.

(4) Robinson, G. W.; Frosch, R. P. *J. Chem. Phys.* **1963**, *38*, 1187.

(5) Pope, M.; Swenberg, C. E. *Electronic Processes in Organic Crystals and Polymers*, 2nd ed.; Oxford Science Publications: Oxford, 1999.

(6) Englman, R. *Non-Radiative Decay of Ions and Molecules in Solids*; North-Holland: Amsterdam, The Netherlands, 1979.

(7) Stein, G.; Würzberg, E. *J. Chem. Phys.* **1975**, *62*, 208.

(8) Cummings, S. D.; Eisenberg, R. *J. Am. Chem. Soc.* **1996**, *118*, 1949.

(9) Siebrand, W. *J. Chem. Phys.* **1967**, *46*, 440.

(10) Beljonne, D.; Cornil, J.; Friend, R. H.; Janssen, R. A. J.; Brédas, J. L. *J. Am. Chem. Soc.* **1996**, *118*, 6453.

(11) Peeters, E.; Ramos, A. M.; Meskers, S. C. J.; Janssen, R. A. J. *J. Chem. Phys.* **2000**, *112*, 9445.

(12) Burin, A. L.; Ratner, M. A. *J. Chem. Phys.* **1998**, *109*, 6092.

(13) Ho, P. K. H.; Kim, J. S.; Burroughes, J. H.; Becker, H.; Li, S. F. Y.; Brown, T. M.; Cacialli, F.; Friend, R. H. *Nature* **2000**, *404*, 481.

(14) Cao, Y.; Parker, I. D.; Yu, G.; Zhang, C.; Heeger, A. J. *Nature* **1999**, *397*, 414.

(15) Shuai, Z.; Beljonne, D.; Silbey, R. J.; Brédas, J. L. *Phys. Rev. Lett.* **2000**, *84*, 131.

(16) Kobrak, M. N.; Bittner, E. R. *Phys. Rev. B* **2000**, *62*, 11473.

(17) Cleave, V.; Yahioglu, G.; Le Barny, P.; Friend, R. H.; Tessler, N. *Adv. Mater.* **1999**, *11*, 285.

(18) Baldo, M. A.; O'Brien, D. F.; You, Y.; Shoustikov, A.; Sibley, S.; Thompson, M. E.; Forrest, S. R. *Nature* **1998**, *395*, 151.

(19) Baldo, M. A.; Thompson, M. E.; Forrest, S. R. *Nature* **2000**, *403*, 750.

(20) Beljonne, D.; Shuai, Z.; Pourtois, G.; Brédas, J. L. *J. Phys. Chem. A*. In press.

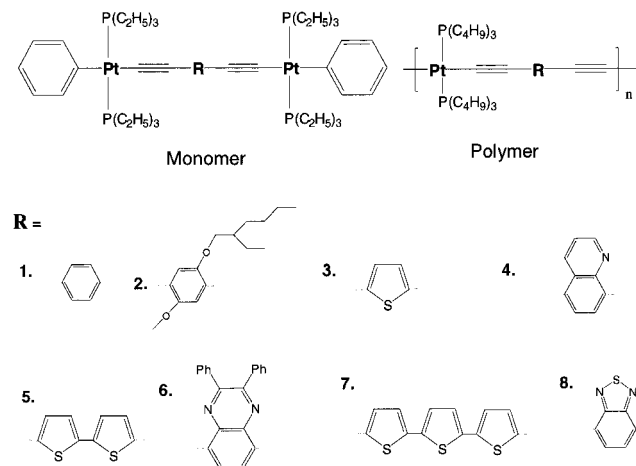


Figure 1. The general chemical structure of the polymers and monomers investigated and the spacer units, R, that were used.

occurs.³ However, this vibrational coupling is not a particularly effective mechanism as a large amount of energy is required to deform the aromatic π -electron cloud.³ For conjugated polymers, the π -electron system is further extended. We therefore consider that it should be even more difficult to deform and that this mechanism of vibronic coupling should be even less effective than for small molecules. Furthermore, there is a higher probability for triplet–triplet annihilation on a polymer chain. As a result, phosphorescence should be extremely difficult to detect in conjugated polymers, and indeed, there are very few reports of their phosphorescence.²¹ Therefore a systematic study of the relationship between the energy of the triplet states and the rate of nonradiative decay has not previously been possible.

Here we have circumvented the problem of the triplet state being nonemissive by using a model system consisting of Pt-containing ethynylene conjugated polymers and monomers of the general form $[-\text{Pt}(\text{PBu}_3)_2-\text{C}\equiv\text{C}-\text{R}-\text{C}\equiv\text{C}-]_n$ for which phosphorescence can be directly observed.^{22–27} Incorporating Pt into the polymer backbone introduces strong spin–orbit coupling while still preserving conjugation.²³ It is therefore possible to access the triplet state by using conventional spectroscopic techniques. The triplet energy level has been tuned between 2.5 and 1.3 eV by varying the spacer R as shown in Figure 1. This has allowed a systematic study of the relationship between triplet energy and the rate of nonradiative decay for a series of conjugated polymers and their corresponding monomers.

II. Experimental Section

The synthesis of the polymers and monomers used for this work is described elsewhere.^{25,28,29} All of the polymers and monomers were

(21) Hertel, D.; Setayesh, S.; Nothofer, H.-G.; Scherf, U.; Müllen, K.; Bäessler, H. *Adv. Mater.* **2001**, *13*, 65.

(22) Wittmann, H. F.; Friend, R. H.; Khan, M. S.; Lewis, J. *J. Chem. Phys.* **1994**, *101*, 2693.

(23) Beljonne, D.; Wittmann, H. F.; Köhler, A.; Graham, S.; Younus, M.; Lewis, J.; Raithby, P. R.; Khan, M. S.; Friend, R. H.; Brédas, J. L. *J. Chem. Phys.* **1996**, *105*, 3868.

(24) Younus, M.; Köhler, A.; Cron, S.; Chawdhury, N.; Al-Mandhary, M. R. A.; Khan, M. S.; Lewis, J.; Long, N. J.; Friend, R. H.; Raithby, P. R. *Angew. Chem., Int. Ed.* **1998**, *37*, 3036.

(25) Chawdhury, N.; Köhler, A.; Friend, R. H.; Wong, W.-Y.; Younus, M.; Raithby, P. R.; Lewis, J.; Corcoran, T. C.; Al-Mandhary, M. R. A.; Khan, M. S. *J. Chem. Phys.* **1999**, *110*, 4963.

(26) Chawdhury, N.; Köhler, A.; Friend, R. H.; Younus, M.; Long, N. J.; Raithby, P. R.; Lewis, J. *Macromolecules* **1998**, *31*, 722.

(27) Wilson, J. S.; Köhler, A.; Friend, R. H.; Al-Suti, M. K.; Al-Mandhary, M. R. A.; Khan, M. S.; Raithby, P. R. *J. Chem. Phys.* **2000**, *113*, 7627.

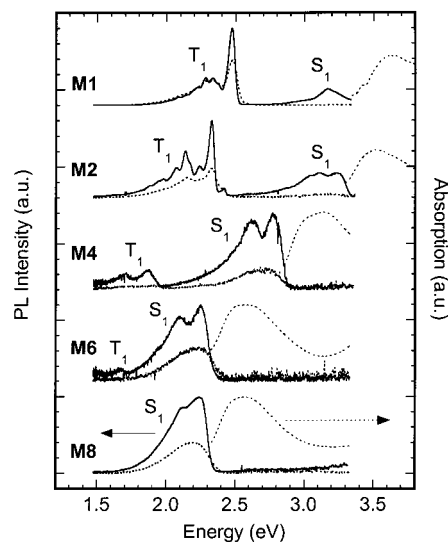


Figure 2. The photoluminescence and absorption spectra of films of monomers **M1**, **M2**, **M4**, **M6**, and **M8**. The absorption spectra are the higher energy dotted lines. PL spectra were taken with UV excitation at both 300 (dotted lines) and 20 K (solid lines). All of the spectra, with the exception of **M1**, give the correct relative intensities for 20 and 300 K. Spectra have been displaced on the vertical axis for clarity.

readily dissolved in dichloromethane at room temperature and thin films of them were produced on quartz substrates by using a conventional photoresist spin-coater. Films were typically 100–150 nm in thickness as measured on a Dektak profilometer. The optical absorption was measured with a Hewlett–Packard ultraviolet–visible (UV–Vis) spectrometer. Measurements of photoluminescence (PL) and photoluminescence lifetimes were made with the sample in a continuous-flow Helium cryostat. The temperature was controlled with an Oxford-Intelligent temperature controller-4 (ITC-4) and a calibrated silicon diode adjacent to the sample. For PL measurements, excitation was provided by the UV lines (334–365 nm) of a continuous wave (cw) Argon ion laser. Typical intensities used were a few mW/mm². The emission spectra were recorded by using a spectrograph with an optical fiber input coupled to a cooled charge coupled device (CCD) array (Oriel Instaspec IV). For the lifetime measurements, the tripled output from a Q-switched YAG laser was used (355 nm, ~15 ns pulses). The emission was recorded by using a photomultiplier tube and a digital oscilloscope. The temporal resolution of this setup was found to be around 70 ns. PL efficiencies were measured by using the integrating sphere technique³⁰ with excitation from a Helium Cadmium laser at 325 nm.

III. Results

A. Absorption and Photoluminescence Spectroscopy. The thin film absorption and photoluminescence spectra of monomers **M1**, **M2**, **M4**, **M6**, and **M8** are shown in Figure 2, and those of polymers **P1–8** are shown in Figure 3. (We refer to the different monomers and polymers shown in Figure 1 by the letters **M** or **P**, respectively, followed by the number of the spacer unit used.) All of the PL spectra (with the exception of monomer **M8**) show two characteristic emission bands. The higher energy band is due to the same singlet excited state as the lowest energy band in the absorption spectra, and denoted by S_1 . (For **P1** and **P2**, the S_1 emission can be seen when using

(28) Davies, S. J.; Johnson, B. F. G.; Khan, M. S.; Lewis, J. *J. Chem. Soc., Chem. Commun.* **1991**, 187.

(29) Khan, M. S.; Al-Mandhary, M. R. A.; Al-Suti, M. K.; Raithby, P. R.; Friend, R. H.; Köhler, A.; Wilson, J. S.; Tedesco, E.; Marsaglia, E. In preparation.

(30) Mello, J. C. d.; Wittmann, H. F.; Friend, R. H. *Adv. Mater.* **1997**, *9*, 230.

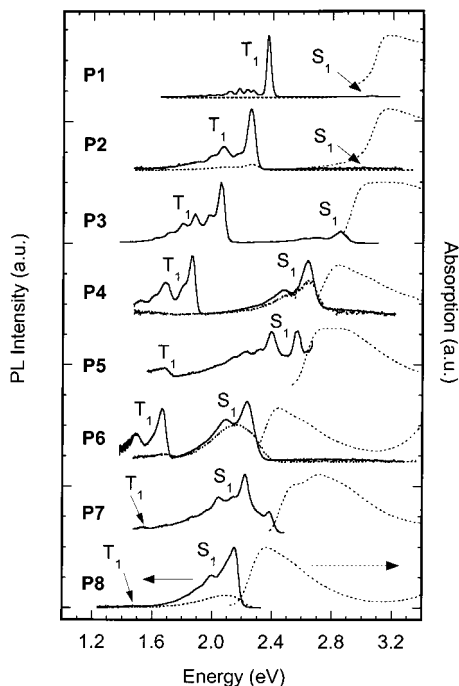


Figure 3. The photoluminescence and absorption spectra of films of polymers **P1–P8**. The absorption spectra are the higher energy dotted lines. PL spectra were taken with UV excitation at both 300 (dotted lines) and 20 K (solid lines). (For polymers **P3**, **P5**, and **P7** only the 20 K spectra are given.) Spectra have been displaced on the vertical axis for clarity.

a suitable scale as previously reported.²⁷) The lower energy emission, denoted by T_1 , is attributed to that of a triplet excited state for the following reasons. The triplet state emission of polymer **P1** has been well-characterized previously²² by lifetime and photoinduced absorption measurements. The lower energy emissions from the other polymers and monomers have similar lifetimes, temperature dependencies, and energies relative to S_1 to those of polymer **P1**.^{25,27–29} In addition, the emissions show vibronic structure and do not change in dilute solutions, which excludes an excimer origin.

The energies of the singlet and the triplet peaks decrease along with the optical gap, and a constant singlet–triplet energy gap of 0.7 ± 0.1 eV is seen for the polymers.^{25,27}

B. Photoluminescence Efficiency Measurements. Photoluminescence quantum yields for the polymers and monomers are given in Table 1. There is no particular trend in the efficiencies of the polymers or monomers apart from an increase when going from the polymer to its corresponding monomer. In general the photoluminescence efficiency reduces as the size of a molecule is increased as a result of a greater number of quenching sites and the possibility of bimolecular decay.⁵

C. Triplet Exciton Lifetime Measurements. The triplet lifetimes in these Pt-containing polymers and monomers are shorter than the few hundred microseconds typically expected for films of poly(phenylene-vinylene)s (PPVs).^{31,32} The spin–orbit coupling introduced by the Pt reduces the triplet state lifetimes since it partially allows transitions between the singlet and triplet manifolds. The emission signals (I) measured over time (t) following excitation from a pulse of laser light for the monomers and polymers at 20 K are shown in Figures 4 and 5. The decaying emission signals have been fitted to exponential curves of the form $I = I_0 \exp(-t/\tau_T) + C$, where I_0 and C are constants, to determine the triplet lifetimes, τ_T , given in Tables

Table 1. The Total Photoluminescence Efficiencies Measured for Polymers **P1–P8** and Monomers **M1**, **M2**, **M4**, **M6**, and **M8**, Using the Integrating Sphere Technique at 300 K

	total photoluminescence efficiency at 300 K/%	
	monomer	
M1		20 ± 2
M2		10 ± 2
M4		5 ± 2
M6		1.1 ± 0.1
M8		12 ± 2
	polymer	
P1		2.2 ± 0.2
P2		6.3 ± 0.3
P3		0.1 ± 0.1
P4		0.32 ± 0.08
P5		0.00
P6		0.24 ± 0.08
P7		0.5 ± 0.5
P8		0.62 ± 0.09

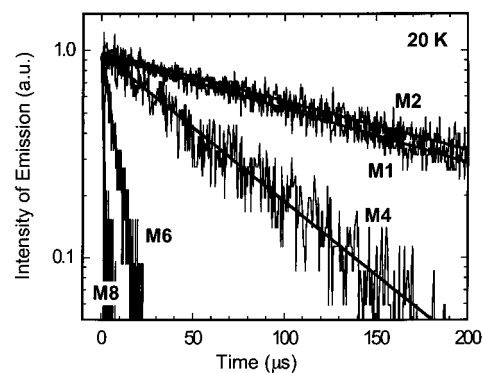


Figure 4. The decaying intensity of triplet emission signals from films of monomers **M1**, **M2**, **M4**, **M6**, and **M8** at 20 K. The laser pulse occurs at $0 \mu\text{s}$ on this time scale and lasts for ~ 15 ns. The fitting curves used to determine the triplet lifetimes are also shown as thick, solid lines.

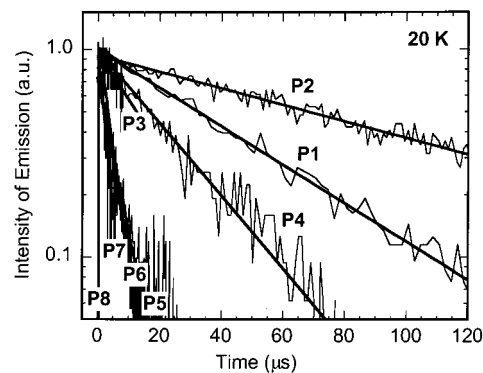


Figure 5. The decaying intensity of triplet emission signals from films of polymers **P1–P8** at 20 K. The laser pulse occurs at $0 \mu\text{s}$ on this time scale and lasts for ~ 15 ns. The fitting curves used to determine the triplet lifetimes are also shown as thick, solid lines.

2 and 3. The lifetimes measured at 300 K are also given in Tables 2 and 3. Lifetimes generally decrease with decreasing triplet energy for both polymers and monomers. No particular trend in lifetimes is seen on comparing polymers and their corresponding monomers.

D. Calculation of the Nonradiative Decay Rate. The above data allow us to calculate the radiative (k_r) and nonradiative (k_{nr}) decay rates. The decay rates are related to the measured lifetime of triplet emission (τ_T), the photoluminescence quantum

Table 2. The Triplet Energies, Measured PL Lifetimes, Phosphorescence Yields, and Radiative and Nonradiative Decay Rates of Monomers **M1**, **M2**, **M4**, **M6**, and **M8** at (a) 20 and (b) 300 K

monomer	$E(T_1-S_0)/\text{eV}$	τ_T at 20 K/ μs	ϕ_P at 20 K	k_{nr} at 20 K/s $^{-1}$	k_r at 20 K/s $^{-1}$
M1	2.48	123 \pm 6	0.2 \pm 0.2	(6 \pm 2) \times 10 3	(2 \pm 2) \times 10 3
M2	2.30	160 \pm 20	0.2 \pm 0.1	(5.0 \pm 0.9) \times 10 3	(1.0 \pm 0.6) \times 10 3
M4	1.85	41 \pm 4	0.03 \pm 0.02	(2.4 \pm 0.2) \times 10 4	(0.7 \pm 0.4) \times 10 3
M6	1.70	11 \pm 3	0.009 \pm 0.007	(9 \pm 2) \times 10 4	(0.8 \pm 0.6) \times 10 3
M8	1.30	2.7 \pm 0.8	0.005 \pm 0.004	(4 \pm 1) \times 10 5	(2 \pm 1) \times 10 3
monomer	$E(T_1-S_0)/\text{eV}$	τ_T at 300 K/ μs	ϕ_P at 300 K	k_{nr} at 300 K/s $^{-1}$	k_r at 300 K/s $^{-1}$
M1	2.48	97 \pm 8	0.2 \pm 0.2	(8 \pm 2) \times 10 3	(2 \pm 2) \times 10 3
M2	2.30	30 \pm 30	0.10 \pm 0.08	(3 \pm 3) \times 10 4	(3 \pm 3) \times 10 3
M4	1.85	23 \pm 3	0.02 \pm 0.01	(4.3 \pm 0.6) \times 10 4	(0.9 \pm 0.5) \times 10 3
M6	1.70	10 \pm 2	0.002 \pm 0.001	(1.0 \pm 0.2) \times 10 5	(0.2 \pm 0.1) \times 10 3
M8	1.30	1.0 \pm 0.1	0.0010 \pm 0.0008	(1.0 \pm 0.1) \times 10 6	(1.0 \pm 0.8) \times 10 3

Table 3. The Triplet Energies, Measured PL Lifetimes, Phosphorescence Yields, and Radiative and Nonradiative Decay Rates of Polymers **P1–P8** at (a) 20 and (b) 300 K

polymer	$E(T_1-S_0)/\text{eV}$	τ_T at 20 K/ μs	ϕ_P at 20 K	k_{nr} at 20 K/s $^{-1}$	k_r at 20 K/s $^{-1}$
P1	2.40	51 \pm 4	0.3 \pm 0.2	(1.4 \pm 0.4) \times 10 4	(6 \pm 4) \times 10 3
P2	2.25	112 \pm 5	0.2 \pm 0.1	(7.1 \pm 0.9) \times 10 3	(1.8 \pm 0.9) \times 10 3
P3	2.05	17 \pm 5	0.02 \pm 0.02	(6 \pm 2) \times 10 4	(1 \pm 1) \times 10 3
P4	1.86	33 \pm 5	0.010 \pm 0.008	(3.0 \pm 0.5) \times 10 4	(0.3 \pm 0.2) \times 10 3
P5	1.67	3.5 \pm 0.2	0.0000	(2.9 \pm 0.2) \times 10 5	0
P6	1.66	2.8 \pm 0.8	0.003 \pm 0.002	(4 \pm 1) \times 10 5	(1.0 \pm 0.8) \times 10 3
P7	1.53	1.8 \pm 0.4	0.0007 \pm 0.0007	(6 \pm 1) \times 10 5	(0.4 \pm 0.4) \times 10 3
P8	1.49	0.18 \pm 0.02	0.0002 \pm 0.0002	(5.6 \pm 0.6) \times 10 6	(1 \pm 1) \times 10 3
polymer	$E(T_1-S_0)/\text{eV}$	τ_T at 300 K/ μs	ϕ_P at 300 K	k_{nr} at 300 K/s $^{-1}$	k_r at 300 K/s $^{-1}$
P1	2.40	—	0.019 \pm 0.002	—	—
P2	2.25	24 \pm 20	0.06 \pm 0.05	(4 \pm 3) \times 10 4	(3 \pm 3) \times 10 3
P3	2.05	—	0.002 \pm 0.002	—	—
P4	1.86	11 \pm 3	0.0006 \pm 0.0006	(9 \pm 2) \times 10 4	(0.05 \pm 0.05) \times 10 3
P5	1.67	1.7 \pm 0.2	0.0000	(5.9 \pm 0.7) \times 10 5	0
P6	1.66	0.4 \pm 0.2	0.0005 \pm 0.0002	(2 \pm 1) \times 10 6	(1 \pm 1) \times 10 3
P7	1.53	0.24 \pm 0.03	0.0007 \pm 0.0007	(4.2 \pm 0.5) \times 10 6	(3 \pm 3) \times 10 3
P8	1.49	0.2 \pm 0.2	0.00010 \pm 0.00008	(5 \pm 5) \times 10 6	(0.5 \pm 0.5) \times 10 3

yield of phosphorescence (Φ_P), and the intersystem crossing efficiency (Φ_{ISC}) by the following expressions:³

$$\tau_T = 1/(k_r + k_{nr}) \quad (1)$$

$$\Phi_P = \Phi_{ISC} k_r \tau_T \quad (2)$$

The measured triplet lifetimes therefore result from a combination of radiative and nonradiative decay rates. The triplet lifetimes τ_T have been measured directly at 20 and 300 K and are given in Tables 2 and 3.

The PL quantum yields for phosphorescence, Φ_P , can be calculated from the overall quantum yields measured at room temperature by considering the fraction of the total photon flux represented by the triplet emission. To determine the low-temperature quantum efficiencies we measured the room temperature efficiencies in an integrating sphere. We then measured the PL in a fixed geometry at 300 and 20 K and scaled the quantum efficiency accordingly. The changes in absorption with temperature at the excitation energy have been measured and accounted for. Values for Φ_P are given in Tables 2 and 3 and are quoted as absolute values rather than percentages.

An expression for the nonradiative decay rate in terms of the triplet lifetime τ_T and phosphorescence efficiency Φ_P can be obtained by combining eqs 1 and 2:

$$k_{nr} = (1 - (\Phi_P/\Phi_{ISC}))/\tau_T \quad (3)$$

The efficiency of intersystem crossing to the triplet state Φ_{ISC} is often assumed to be unity for second and third row transition

metal chromophores based on early work by Demas and Crosby on Ru and Os.^{8,33} This assumption has been confirmed for polymer **P1** by Wittmann et al.²² The fraction of singlets undergoing intersystem crossing in a compound, Φ_{ISC} , is determined by the amount of spin-orbit coupling and the energy gap between S_1 and T_1 . The spin-orbit coupling scales as Z^4 for atoms so it should be entirely controlled by the platinum atom in these materials, and in addition the S_1-T_1 energy gap is constant at around 0.7 eV for the polymers^{25,27} and 0.9–0.7 eV for the monomers. It should therefore be reasonable to assume Φ_{ISC} is constant and close to unity for the rest of the series too. This gives

$$k_{nr} = (1 - \Phi_P)/\tau_T \quad (4)$$

$$k_r = \Phi_P/\tau_T \quad (5)$$

Values calculated for k_r and k_{nr} for the polymers and monomers are given in Tables 2 and 3. These values represent the averages obtained from a number of measurements and the corresponding statistical errors are also given. Since Φ_P is small, from eq 4, it can be seen that trends in k_{nr} are mostly determined by those observed for τ_T .

We note that if one wished to explain the trends seen in k_{nr} by a varying Φ_{ISC} , this would require Φ_{ISC} to decrease by 3 orders of magnitude, which seems unlikely.

(31) Ginger, D. S.; Greenham, N. C. *Phys. Rev. B* **1999**, *59*, 10622.
 (32) Partee, J.; Frankevich, E. L.; Uhlhorn, B.; Shinar, J.; Ding, Y.; Barton, J. T. *Phys. Rev. Lett.* **1999**, *82*, 3673.
 (33) Demas, N. J.; Crosby, G. A. *J. Am. Chem. Soc.* **1970**, *92*, 7262.

IV. Discussion

A. The Energy Gap Law. The energy gap law relates the nonradiative decay rate of a transition to the energy gap between the states involved.⁵ In its simplest form, it may be written as:

$$k_{\text{nr}} \propto \exp(-\gamma\Delta E/\hbar\omega_{\text{M}}) \quad (6)$$

where ΔE is the energy gap separation between the potential minima of the states involved, γ is a term that can be expressed in terms of molecular parameters, and ω_{M} is the maximum and dominant vibrational frequency available in the system. For a system with several high-frequency modes a corresponding weighted term is used.⁵

This relationship arises from the vibrational overlap of the two states so that the nonradiative decay rate becomes a function of the Franck–Condon factor and of the vibrationally induced electronic coupling term,⁴

$$k_{\text{nr}} = (2\pi/\hbar)\beta^2 F\rho \quad (7)$$

where β is the energy of interaction between the initial and final states (for the T_1-S_0 transition in the Pt-containing materials this corresponds to the spin–orbit coupling), ρ is the number of states per unit energy, and F is the Franck–Condon factor at the appropriate energy. The mechanism of nonradiative decay upon which the energy gap law is based is therefore intrinsically linked to the electron–lattice coupling of the material.

For aromatic hydrocarbons, eq 7 has been applied to triplet to ground state transitions. An approximately exponential decrease in F with increasing ΔE has been calculated,² thus relating eqs 6 and 7. For a specific transition in a class of related molecules $F(E)$ is presumed to be the only parameter that varies appreciably.

The energy gap law has also been applied to some Pt, Ru, and Os complexes.⁸ Furthermore, it is seen that the emission of trivalent ions of Pr, Sm, Eu, Gd, Tb, Dy, and Tm in H_2O and D_2O is dependent on the gap between the highest fluorescent and lowest nonfluorescent levels.⁷

For our Pt-containing polymers and monomers, we have plotted $\ln(k_{\text{nr}})$ against ΔE_{ST} , where ΔE_{ST} is ΔE for the T_1-S_0 transition, and fitted the data to straight lines for both room temperature and 20 K measurements (Figure 6). We obtain good fits for the monomers and reasonable fits for the polymers. According to eq 6, the gradients of the plots are given by $\gamma/\hbar\omega_{\text{M}}$ and are therefore controlled by the molecular parameters and vibrational modes. For our polymers and monomers, we find gradients of -6 ± 1 and $-3.8 \pm 0.5 \text{ eV}^{-1}$, respectively. These are similar to the slopes found for Pt, Os, and Ru complexes.⁸ We would expect to find similar gradients since the vibrational modes in the organic chromophores involved are of similar energies. According to eq 6, the absolute values of k_{nr} depend on a preexponential factor. The values we obtain for our Pt-containing materials (Tables 2 and 3) lie between those found for Pt(II) complexes and those found for hydrocarbon molecules.^{5,8} On the basis of our results we therefore consider that the nonradiative decay of Pt-containing polymers and monomers can be described by the energy gap law.

The values we obtained for k_{r} are given in Tables 2 and 3 and are around 10^3 s^{-1} for both polymers and monomers. For phosphorescence in aromatic hydrocarbon molecules, k_{r} is typically found to be between 0.1 and 1 s^{-1} .³ So, the spin–orbit coupling introduced by the Pt in our polymer and monomer structures increases the radiative decay rate for phosphorescence by up to 4 orders of magnitude. We note, however, that this is

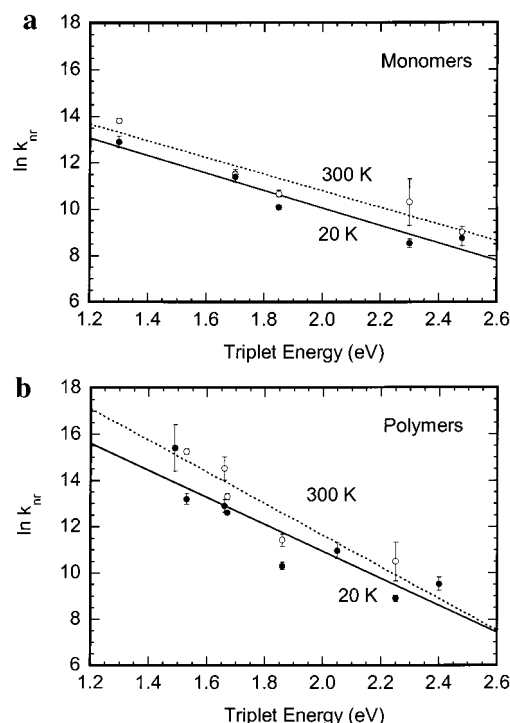


Figure 6. (a) The natural log of the nonradiative decay rate plotted against triplet energy (T_1-S_0) for monomers **M1**, **M2**, **M4**, **M6**, and **M8**. The dotted line is the best fit straight line for data at 300 K and the solid line the best fit for 20 K. The 20 K data points are closed circles and the 300 K data points are open circles. (b) The natural log of the nonradiative decay rate plotted against triplet energy (T_1-S_0) for polymers **P1–P8**. The dotted line is the best fit straight line for data at 300 K and the solid line the best fit for 20 K. The 20 K data points are closed circles and the 300 K data points are open circles.

still small compared to the fully allowed singlet transitions which have radiative decay rates of 10^7-10^8 s^{-1} .³ Comparing the k_{r} and k_{nr} values for the individual Pt-containing polymers and monomers it can be seen that the values for the nonradiative decay rate, k_{nr} , are only small enough to be comparable to the radiative decay rate, k_{r} , for materials with T_1-S_0 gaps of 2.4 eV or above. This corresponds to S_1-S_0 gaps of 3.0 eV or higher.

B. Mechanisms of Nonradiative Decay. The energy gap law for nonradiative decay (eq 6) includes the term ω_{M} , which is the maximum vibrational frequency available in the system. The larger ω_{M} is, the greater the nonradiative decay rate becomes. This has been explained by considering the primary mechanism for nonradiative decay to be a release of energy from the excited state to the surroundings through the vibration of bonds within the molecule allowing the molecule to return to the ground state.^{2,5} This mechanism of multiphonon emission will be most efficient for the vibrations in the molecule that have the largest ω_{M} and which therefore require the fewest quanta to carry off a given amount of energy. For aromatic hydrocarbons this is often the C–H stretching mode with a vibrational frequency of 0.37 eV.^{2,34} Meanwhile, for many transition metal diimine complexes the dominant acceptor vibration has been attributed to a ring-stretching mode of 0.16 eV that is observed from the progression in the structure of the 77 K emission profile.^{35–37}

(34) Siebrand, W.; Williams, D. F. *J. Chem. Phys.* **1967**, *46*, 403.

(35) Caspar, J. V.; Kober, E. M.; Sullivan, B. P.; Meyer, T. J. *J. Am. Chem. Soc.* **1982**, *104*, 630.

(36) Kober, E. M.; Caspar, J. V.; Lumpkin, R. S.; Meyer, T. J. *J. Phys. Chem.* **1986**, *90*, 3722.

(37) Caspar, J. V.; Meyer, T. J. *J. Am. Chem. Soc.* **1983**, *105*, 5583.

It is not yet possible to comment upon which modes of nonradiative decay are most active in all the Pt-containing polymers and monomers investigated here. Yet the Raman spectra of polymer **P1** identify four normal modes at 0.103, 0.145, 0.198, and 0.261 eV.²³ These have previously been assigned to a C–H bending mode, and stretching modes of the C–C, benzene, and C≡C groups, respectively. The Raman active modes of conjugated polymers couple directly to the π bond order along the chain, and are therefore strongly coupled to excited electronic states. We consider that the high-energy benzene and C≡C stretching modes will be particularly efficient at promoting nonradiative decay in this material.

C. Comparison of Polymers and Monomers. Previous investigations of nonradiative decay have tended to be for organic molecules,² rare earth ions,⁷ and metal complexes.⁸ Here we have been able to derive values of k_{nr} not only for a series of monomers, but also for the corresponding series of polymers. The nonradiative decay of large conjugated systems, such as our polymers, has not previously been addressed in the context of the energy gap law. We now compare the nonradiative decay of Pt-containing polymers with that of their monomers.

Despite the fact that the same organic groups are available for nonradiative decay in the polymers and corresponding monomers, it is possible to identify several factors which may give rise to different nonradiative behavior. First, comparing the PL spectra of monomers and their corresponding polymers (Figures 2 and 3), it can be seen that there is consistently more weight in the vibronic side peaks of the monomers' triplet emission than in the polymers' triplet emission. This indicates that there is less overlap between the vibrational levels of the ground and excited states, and therefore that the triplet excited state in the monomer is more distorted than the triplet state in the polymer.³ Calculations performed for polymer **P1** and monomer **M1** have also shown this to be the case for these two materials.²³ Second, since it may be possible for triplets to diffuse along a polymer chain, there may be bimolecular nonradiative decay mechanisms such as triplet–triplet annihilation³² operational for the polymer which cannot occur in the monomer. From Figure 6a,b it can be seen that, within the limits of experimental error shown, the polymers and corresponding monomers appear to have similar k_{nr} values. This is consistent with the fact that the site of emission and thus the vibrations involved are the same. It also suggests that any bimolecular quenching processes in the polymers play a lesser role than the vibrationally induced nonradiative decay.

When considering the gradients of Figure 6a,b, it was noted that the gradient of $\ln(k_{nr})$ against ΔE_{ST} for the polymers was $-6 \pm 1 \text{ eV}^{-1}$ compared to $-3.8 \pm 0.5 \text{ eV}^{-1}$ for the monomers. According to the energy gap law, the gradients of the plots should be equal to $-\gamma/\hbar\omega_M$. Since the vibrations involved in

the nonradiative decay of the triplet on the monomer and on the polymer are believed to be the same, then it must be a different factor γ that results in the two gradients. In fact, γ varies with the displacement of the potential energy surface minima, Δ_M , for the two states involved in the transition.¹ According to Englman et al.,¹ increasing Δ_M results in a decrease in γ . The smaller gradient for the monomer is therefore consistent with the greater distortion of the triplet in the monomer than in the polymer.

V. Conclusions

In contrast to the fully allowed optical transitions for the singlet states, triplet state emission in conjugated polymers is at best only partially allowed and therefore has a long lifetime in the range of microseconds^{31,32} to seconds.^{11,21} For this reason the decay of triplet states is controlled by nonradiative mechanisms. These same nonradiative decay mechanisms also apply to the singlet states but are often insignificant in comparison to the fast radiative decay or intersystem crossing.

This work shows that the nonradiative decay of the triplet states in a series of Pt-containing conjugated polymers and monomers may be quantitatively described by the energy gap law. The nonradiative decay rate is very sensitive to the triplet energy, increasing exponentially as the triplet energy decreases. Our results therefore imply that high-energy triplet states intrinsically have the most efficient phosphorescence.

The mechanism for nonradiative decay inherent to the energy gap law is multiphonon emission through the vibration of bonds on the conjugated organic spacer groups. Since this mechanism is associated with the conjugated organic unit, rather than the Pt, we consider that the energy gap law may also be applied to other conjugated polymers. It has already been shown that the triplet state in LEDs may be utilized through light-harvesting techniques.^{17,19} To optimize this technique our results clearly imply that work should focus on polymers with high energy triplets (and concurrently high optical gaps) to avoid competition with nonradiative decay. In addition, suppression of the high-energy vibrational modes by chemical design of rigid polymers should decrease nonradiative decay rates.

Acknowledgment. A.K. thanks Peterhouse, Cambridge, for a Fellowship and the Royal Society for a University Research Fellowship. M.S.K. gratefully acknowledges Sultan Qaboos University (SQU), Oman for a research grant, SQU/SCI/CHEM/1999/02, and thanks EPSRC (UK) for a Visiting Fellowship and SQU for research leave. We would like to thank CDT Ltd. for assistance with photoluminescence efficiency measurements. This work was funded by the EPSRC.

JA010986S